Pharm Res (2014) 31:1907–1918
DOI 10.1007/s11095-013-1292-0

RESEARCH PAPER

Saturated Long-Chain Esters of Isopulegol as Novel Permeation Enhancers for Transdermal Drug Delivery

Yang Chen • Dongmei Cun • Peng Quan • Xiaochang Liu • Wenjia Guo • Lihua Peng • Liang Fang

Received: 2 August 2013 / Accepted: 31 December 2013 / Published online: 22 January 2014

ABSTRACT

Purpose Saturated long-chain esters of isopulegol were synthesized and their activities as permeation enhancers for transdermal delivery of amlodipine and flurbiprofen were investigated, in contrast to the saturated fatty acids and isopulegol, as well as their physical mixtures.

Methods *In vitro* permeation experiments, confocal laser scanning microscopy (CLSM) and attenuated total reflection Fourier transform infrared (ATR-FTIR) spectroscopy were introduced to investigate the regulation of enhancers in the skin permeability and biophysical properties. With *in vitro* cytotoxicity test and *in vivo* erythema model, the skin irritation of enhancers was evaluated.

Results The esters significantly increased the permeation of amlodipine and flurbiprofen, whereas saturated fatty acids and isopulegol had no such effect and even decreased the drug permeation when they were used alone or in combination. These results were supported by CLSM and ATR-FTIR studies, which revealed that only the esters could decrease the order of the alkyl chains in the skin lipids. Additionally, almost no skin irritation and cytotoxicity were observed for these esters.

Conclusions Saturated long-chain esters of isopulegol are shown to be suitable permeation enhancers for transdermal drug delivery. Covalent attachment of isopulegol and saturated fatty acids might represent a promising strategy to design novel and potent permeation enhancers.

Electronic supplementary material The online version of this article (doi:10.1007/s11095-013-1292-0) contains supplementary material, which is available to authorized users.

Y. Chen • D. Cun • P. Quan • X. Liu • W. Guo • L. Fang (✉)
Department of Pharmaceutical Science, School of Pharmacy
Shenyang Pharmaceutical University, 103 Wenhua Road
Shenyang, Liaoning 110016, China
e-mail: fangliang2003@yahoo.com

L. Peng (✉)
Institute of Pharmaceutics, College of Pharmaceutical Sciences
Zhejiang University, 866 Yuhangtang Road
Hangzhou, Zhejiang 310058, China
e-mail: lhpeng@zju.edu.cn

KEY WORDS isopulegol · permeation enhancer · saturated fatty acid · saturated long-chain ester · transdermal drug delivery

ABBREVIATIONS

ATR-FTIR	Attenuated total reflection Fourier transform infrared spectroscopy
AM	Amlodipine
CLSM	Confocal laser scanning microscopy
DA	Decanoic acid
ER	Enhancement ratio
FP	Flurbiprofen
HA	Hexanoic acid
ISO	Isopulegol
ISO-Cn	Long-chain esters of isopulegol
LA	Lauric acid
MA	Myristic acid
MTT	3-(4, 5-dimethylthiazol-2-yl)-2, 5-diphenyltetrazolium bromide
OA	Octanoic acid
PA	Palmitic acid
SDS	Sodium dodecyl sulfate
SC	Stratum corneum
TDDS	Transdermal drug delivery system

INTRODUCTION

Transdermal drug delivery has been accepted as a potential non-invasive route of administration, with advantages of prolonged therapeutic action, decreased side effect, easy use and better patient compliance. Despite its great potential, delivery of many molecules via this route remains one of the major challenges in the development of drug delivery systems. This is mainly due to the instinct barrier function of the skin, provided by the highly organized structure of the stratum corneum (SC) (1).

An approach commonly researched to increase the permeability through the skin has been to incorporate permeation enhancers into formulations. To date, hundreds of structurally different chemicals have been evaluated for their permeation enhancing activities. In spite of the extensive research in this field, novel enhancers such as Transkarbam 12 (2) and amino acid esters (3) with high efficiency and safety are scarce, and the action of permeation enhancers has still been poorly understood (4).

Many permeation enhancers possess a long hydrophobic chain and a cyclic head in their structures. Compounds such as azone (5), tranexamic acid esters (6) and cyclohexanol derivatives (7), all belong to this category. It is hypothesized that these molecules are likely to be effectively inserted into the lipid lamellae in the SC, with their polar heads in the polar region and the long hydrophobic chain between the alkyl tails of the interculluar lipids. Such interaction would induce the disturbance of lipid packing, lateral fluidization and decrease of the skin barrier resistance (8). Therefore, chemical attachment of a long hydrophobic chain to a cyclic molecule containing polar functional groups might be a promising strategy to design novel and potent permeation enhancers.

Isopulegol (ISO) is one kind of cyclic terpenes, and has been shown effective in promoting the percutaneous absorption of various drugs with low skin irritation (9). However, application of ISO in transdermal drug delivery systems would be hindered by its undesirable odor and high volatility. To address these issues and further to identify more potent permeation enhancers in this study, the saturated long-chain esters of ISO were synthesized via the esterification reaction between ISO and saturated fatty acids, which was another kind of widely used permeation enhancers (10). As the combination of different permeation enhancers might induce synergistic effect higher than that when they were used alone (11), the efficacy of physical mixtures of saturated fatty acids and ISO in permeation enhancement was also investigated.

The purpose of this study was to explore the feasibility of saturated long-chain ISO esters for use as permeation enhancers, and to investigate their advantages in transdermal enhancement by comparison with saturated fatty acids and ISO. Flurbiprofen (FP) and amlodipine (AM) were used as two model drugs with different physicochemical properties to evaluate the enhancing efficiency of the studied compounds. With the confocal laser scanning microscopy (CLSM) and attenuated total reflection Fourier transform infrared spectroscopy (ATR-FTIR) analysis, the regulation and the underlying action mechanisms of these chemicals in the skin microstructures, including the barrier properties of SC and the conformational order of the intercellular skin lipids were respectively investigated. In addition, with *in vitro* skin cells and *in vivo* rabbit erythema models, the skin irritation and toxicity of the synthesized chemicals were also evaluated.

MATERIALS AND METHODS

Materials

AM besylate and FP were respectively purchased from Jilin Tianfeng Pharmaceutical Co., Ltd. (Jilin, China) and Shanghai Haiqu Chemical Co., Ltd. (Shanghai, China). ISO (purity>85%) was bought from TCI (Tokyo, Japan), and used in the study after further purification (> 98%). Saturated fatty acids were provided by Aladdin Reagent Co., Ltd. (Beijing, China). Propylparaben (purity>99%) and isopropyl myristate (IPM) were both purchased from China National Medicines Co., Ltd. (Shanghai, China). Fluorescein was provided by AXROS Organics (New Jersey, USA). Methanol of HPLC grade was obtained from Yuwang Pharmaceutical Co., Ltd. (Shandong, China). All of other chemical reagents were of at least reagent grade available.

Preparation of AM from AM Bensylate

AM was prepared from its bensylate salt using an acid-base titration and extraction procedure as previously reported by us (12). The prepared product was identified as highly pure (> 99.5%) by the area normalization method of HPLC.

Synthesis of the Long-Chain Esters of ISO

The reaction sequences for preparing long-chain esters of ISO were illustrated in Fig. 1. Generally, 0.016 mol saturated fatty acids, including hexanoic acid (HA), octanoic acid (OA), decanoic acid (DA), lauric acid (LA), myristic acid (MA) or palmitic acid (PA), were dissolved in thionyl chloride and heated to reflux for 3 h. Then, the surplus solvent was evaporated at reduced pressure. ISO (0.013 mol) dissolved in tetrahydrofuran was added into the reaction solution, and stirred at 60°C for 2.5 h. After reaction, tetrahydrofuran was evaporated in vacuum and the residue was taken up in ethyl acetate. A solution of NaOH (10%, w/v) was added to adjust the pH to 5–6. Then, the organic layer was separated, successively washed with pure water and brine, dried with anhydrous Na_2SO_4, and finally freed of volatile solvent under vacuum. The residue was purified by silica gel column chromatography using a mixture of petroleum and ethyl acetate (200:1→70:1) to afford the product as colorless oil (TLC: Rf=0.6 with 20:1 petroleum and ethyl acetate). The purity of each compound was over 98%, as determined

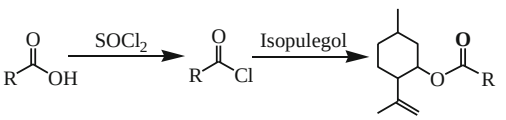

Fig. 1 Synthesis scheme of ISO esters, i.e. ISO-Cn (n=6, 8, 10, 12, 14, 16).

by gas chromatography (GC-14C, Shimadzu, Japan). Their structures were characterized with ^{1}H-NMR and GC-MS.

ISO-C6

^{1}H-NMR (300 MHz, $CDCl_3$): δ 4.798 (1H, m, -OCH), 4.717 (s, 2H, $=CH_2$), 2.244 (t, 2H, $-COCH_2$, J= 7.5 Hz), 2.099 (m, 1H, -CH), 2.060 (m, 1H, -CH), 1.655 (m, 8H, 4 $-CH_2$), 1.270 (m, 5H, $-CH_2$, $-CH_3$), 0.904 (m, 8H, 2 $-CH_3$, $-CH_2$); GC-MS m/z:252.3 [M^+]. Yield: 61%.

ISO-C8

^{1}H-NMR (300 MHz, $CDCl_3$): δ 4.798 (1H, m, -OCH), 4.718 (s, 2H, $=CH_2$), 2.221 (t, 2H, $-COCH_2$, J= 7.5 Hz), 2.132 (m, 1H, -CH), 2.005 (m, 1H, -CH), 1.656 (m, 8H, 4 $-CH_2$), 1.264 (m, 9H, 3 $-CH_2$, $-CH_3$), 0.904 (m, 8H, 2 $-CH_3$, $-CH_2$); GC-MS m/z:280.3 [M^+]. Yield: 58%.

ISO-C10

^{1}H-NMR (300 MHz, $CDCl_3$): δ 4.799 (1H, m, -OCH), 4.720 (d, 2H, $=CH_2$), 2.222 (t, 2H, $-COCH_2$, J= 7.5 Hz), 2.106 (m, 1H, -CH), 2.007 (m, 1H, -CH), 1.656 (m, 8H, 4 $-CH_2$), 1.264 (m, 13H, 5 $-CH_2$, $-CH_3$), 0.904 (m, 8H, 2 $-CH_3$, $-CH_2$); GC-MS m/z:308.4 [M^+]. Yield: 53%.

ISO-C12

^{1}H-NMR (300 MHz, $CDCl_3$): δ 4.798 (1H, m, -OCH), 4.720 (d, 2H, $=CH_2$), 2.220 (t, 2H, $-COCH_2$, J= 7.5 Hz), 2.103 (m, 1H, -CH), 1.967 (m, 1H, -CH), 1.653 (m, 8H, 4 $-CH_2$), 1.255 (m, 17H, 7 $-CH_2$, $-CH_3$), 0.902 (m, 8H, 2 $-CH_3$, $-CH_2$); GC-MS m/z:336.3 [M^+]. Yield: 58%.

ISO-C14

^{1}H-NMR (300 MHz, $CDCl_3$): δ 4.798 (1H, m, -OCH), 4.721 (d, 2H, $=CH_2$), 2.222 (t, 2H, $-COCH_2$, J= 7.5 Hz), 2.103 (m, 1H, -CH), 1.967 (m, 1H, -CH), 1.657 (m, 8H, 4 $-CH_2$), 1.255 (m, 21H, 9 $-CH_2$, $-CH_3$), 0.893 (m, 8H, 2 $-CH_3$, $-CH_2$); GC-MS m/z:364.4 [M^+]. Yield: 55%.

ISO-C16

^{1}H-NMR (300 MHz, $CDCl_3$): δ 4.799 (1H, m, -OCH), 4.720 (d, 2H, $=CH_2$), 2.221 (t, 2H, $-COCH_2$, J= 7.5 Hz), 2.105 (m, 1H, -CH), 1.972 (m, 1H, -CH), 1.655 (m, 8H, 4 $-CH_2$), 1.254 (m, 25H, 9 $-CH_2$, $-CH_3$), 0.892 (m, 8H, 2 $-CH_3$, $-CH_2$); GC-MS m/z:392.4 [M^+]. Yield: 49%.

Volatilization of ISO and the Long-Chain Esters

The weight loss method was employed to determine the volatilization rates of ISO and its esters. Briefly, an excessive amount of ISO or its esters were placed at 50°C in the crucible, and the total weight was determined at predetermined time intervals over a period of 6 h. The cumulative amount of enhancer losing per unit area was plotted against time. The slope of the plot gave the volatilization rate.

Skin Preparation

Male Wistar rats (180–220 g, 6–8 weeks old) were supplied by the Experimental Animal Center of Shenyang Pharmaceutical University (Shenyang, China). All the animal procedures were performed in accordance with the NIH Guidelines for the Care and Use of Laboratory Animals and also in accordance with the guidelines for animal use published by the Life Science Research Center of Shenyang Pharmaceutical University. During the experiments, the rats were anesthetized with urethane (20% w/v, i.p.), and hair on the abdominal area was removed first by trimming with an electric clipper and then by shaving with a razor. The barrier function of the skin was then checked *in vivo* by measuring its transepidermal water loss using an open-chamber Tewameter® (TM 300, Courage & Khazaka Co., Germany), and the skin showing water permeation rate ranging from 4.0 $g \cdot m^{-2} \cdot h^{-1}$ to 8.0 $g \cdot m^{-2} \cdot h^{-1}$ were chosen for further treatment (13). After that, the full-thickness skins (i.e. epidermis with SC and dermis) were excised from the shaved abdomen sites of the sacrificed rats. The adhering subcutaneous fat and other extraneous tissue were carefully removed from the under surface with tweezers. The integrity of the skin was carefully ascertained by microscope observation, and any skin with low uniformity was rejected. Finally, the skin was wrapped in aluminum foil and stored at −70°C until use. Prior to each experiment, the skin segments were allowed to thaw slowly in order to avoid damage.

Preparation of the Donor Solutions

The donor solutions used for percutaneous experiments were prepared as follows. First, 2 mmol each of the tested compounds was added in IPM (12 g), and a slight heating (up to 50°C) might be used for a rapid dissolution. Excess amounts of drug were then added into the formulation, followed by sonication for 10 min and equilibration overnight. Control samples were obtained in a similar way without addition of any enhancers.

In Vitro Permeation Experiments

Two-chamber diffusion cells with an effective diffusion area of 0.95 cm^2 were used for the permeation study. Briefly, the isolated full-thickness skin was mounted between the diffusion cells with the epidermis facing towards the donor compartment. Then donor solution of 4 mL was applied in the donor compartment, and an equal volume of phosphate buffered saline (PBS, pH 7.4) was added into receptor compartment. The cells were maintained at 32°C and stirred with magnetic bars. At the predetermined time intervals (1, 2, 3, 4, 5, 6, 7, 8 h), receptor solution of 2 mL was withdrawn and replaced with the same volume of fresh receptor solution. Samples were analyzed by HPLC after the centrifugation and appropriate dilution. The experiments were performed in quadruplicates using the skin from four different rats.

Determination of Drug Solubility in the Donor Vehicle

Excess amounts of FP or AM were dispersed in the donor solution with or without enhancers. The suspensions were shaken vigorously for 48 h in a water bath at 32±1°C. Finally the suspensions were filtered through a 0.45-μm millipore filter, diluted with methanol before determination. The experiments were performed in quadruplicates.

HPLC Analysis

An HPLC apparatus equipped with an L-2420 variable-wavelength ultraviolet absorbance detector and an L-2130 pump (Hitachi High-Technologies Corporation, Tokyo, Japan) were used to measure the drug concentrations. Analyses were performed on a 5-μm ODS column (20 cm×4.6 mm, Dikma Technologies, Beijing, China) at 40°C. The mobile phase of AM consisted of methanol and 0.03 mol/L KH_2PO_4 buffer solution (7:3, v/v). The wavelength of detector was 238 nm (12). The mobile phase of FP consisted of methanol, water and acetic acid (3: 1: 0.005, v/v), and the pH was adjusted to 5.99 with triethylamine. The wavelength for detection was set at 245 nm (14). The flow rate was set as 1 mL/min, and propylparaben (10 μg/mL) was used as the internal standard under the above two conditions. AM and internal standard were separately eluted at the retention times of 4.55 min and 5.60 min, with the resolution of 2.58. Limits of detection and quantification of AM were 0.05 μg/mL and 0.15 μg/mL, respectively. FP and internal standard were separately eluted at the retention times of 4.50 min and 6.30 min, with the resolution of 4.89. Limits of detection and quantification of FP were 0.15 μg/mL and 0.40 μg/mL, respectively.

Data Analysis

The amount of drug penetrated across the skin was calculated based on the measured receptor phase concentration and the sampling effects. The cumulative penetrated amount per unit area (Q_{8h}, $\mu g \cdot cm^{-2}$) *versus* time was plotted. The slop and x-intercept of the linear portion of the plot was presented as flux (J_s, $\mu g \cdot cm^{-2} \cdot h^{-1}$) and lag time ($T_{lag}$, h), respectively. Enhancer activity was expressed as enhancement ratio (*ER*), which is the ratio of Q_{8h} in the enhancer group to that in the control group.

The permeability coefficient (P), vehicle/SC partition coefficient (K) and diffusion coefficient (D) were calculated as,

$$P = J_s / C_s \tag{1}$$

$$K = 6 J_s T_{lag} / (H C_s) \tag{2}$$

$$D = H^2 / (6 T_{lag}) \tag{3}$$

where C_s is the drug solubility in donor vehicle, and H is the diffusion path length.

Since most molecules permeated through the SC mainly by a tortuous intercellular route, the thickness of the skin was not equal to the diffusion pathlength. However, it was difficult to determine the path length exactly. Therefore, the partition coefficient (K) and diffusivity (D) were normalized as K' (KH) and D' (D/H^2), respectively, and these parameters could be obtained from the following equations (15):

$$K' = 6 J_s T_{lag} / C_s \tag{4}$$

$$D' = 1 / (6 T_{lag}) \tag{5}$$

Confocal Laser Scanning Microscopy (CLSM)

Saturated fluorescein solution was used in the CLSM analysis. As described in preparation of donor vehicles, the enhancer containing IPM solutions were first prepared. An excess amount of fluorescein was then added to the formulation, followed by sonication for 10 min. The suspensions were centrifuged at 5,000 rpm for 5 min, and the supernatants were subsequently filtered through a 0.45-μm millipore filter. The control sample was obtained in a similar way without addition of any enhancer.

Full thickness rat skin was mounted in the Franz diffusion cells. The donor cells were placed with 200 μL fluorescein

solution, while the receptor cells were filled with PBS. After skin exposure for 20 min, the excess solution was removed from the skin surface, and then the diffusion cells were dismantled. The SC surface of the skin was thoroughly wiped with distilled water before drying gently with filter paper. The skin segment was immediately sandwiched between a glass slide and a coverslip, and examined microscopically without additional tissue processing.

An LSM 710 Laser Scan Microscope (Carl Zeiss Carl Zeiss, Jena, Germany) was used for imaging of the skin samples. The fluorescein was excited using an argon laser at a wavelength of 488 nm. Z stacks of the skin samples were taken from the SC to the dermis. To visualize the distribution of fluorescein, confocal images were first obtained in the xy-plane (i.e., parallel to the plane of the skin surface). The skin surface ($z=0$ μm) was defined as the imaging plane of flurescence with a morphology characteristic of the SC surface. To generate an xz-section, a horizontal line was "drawn" across a region of interest in the $z=0$ μm-xy-plane and then "optically sliced" through the digitized image data of the successive xy-sections to generate xz-planar optical cross-sections (16).

ATR-FTIR Experiments

The rats were first anesthetized with urethane (20% w/v, i.p.) and the abdominal hair was carefully shaved. Ten microliter each enhancer solution (0.065 mmol dissolved in 100 μL ethanol) was spread uniformly over the shaved abdominal area (1×1 cm^2) for an exposure time of 30 min. Skin treated with solvent alone was determined as control. After treatment, the skin was gently blotted with tissue paper and dried at room temperature for 15 min. Then the treated skin segments were excised and determined by an ATR-FTIR spectroscopy (Thermo Nicolet NEXUS 470, Madison, USA). The internal reflection crystal was zinc selenide (ZnSe) set at an incidence angle of 45°. The spectra were obtained as an average of 32 scans recorded between 4,000 cm^{-1} and 1,000 cm^{-1} at a resolution of 2 cm^{-1}. The peak position was analyzed using OMNIC software.

In Vitro Skin Cells Cytotoxicity Assays

The keratinocytes and fibroblasts in the viable skin layers play important roles in the initiation, modulation and regulation of skin inflammation (17). The present cytotoxicity studies were performed on human skin fibroblasts (HSF) or keratinocytes (HaCaT) cell lines using the 3-(4, 5-dimethylthiazol-2-yl)-2, 5-diphenyltetrazolium bromide (MTT, Sigma, USA) assay. HaCaT and HSF were purchased from China Center for Type Culture Collection (Shanghai, China), and were cultured to confluence in Dulbecco's modified Eagle's medium (DMEM; LifeTechnologies, USA) containing 10% fetal bovine serum (FBS;LifeTechnologies, USA), penicillin (100 U/mL; LifeTechnologies, USA) and Roswell Park Memorial Institute 1640 (RPMI; life Technologies, containing 10% FBS and penicillin (100 U/mL), respectively. Cell viability was determined after 24 h treatment with different permeation enhancers at various concentrations (0–3 mmol/L) in 96-well plates. The relative amount of viable cells was determined by measuring the reduction of MTT dye in live cells to blue formazan crystals at optical density at 570 nm and expressed as the percentage of solvent control samples without enhancer treatment.

In Vivo Skin Erythema Analysis

Visual observation of erythema has been widely used to evaluate the irritant potential of substances. However, this method is subjective and imprecise, especially regarding comparisons between the intensities of developed Erythema (18). In order to quantify and compare skin irritation *in vivo*, Mexameter® (MX 16, Courage & Khazaka Co., Germany) was introduced in the present study to determine the erythema index (EI) of the skin. It is non-invasive and involves only one investigator, instead of several trained judges for visual scoring.

According to the guideline of CIE (Commission International de l'Eclairage), rabbit were used to assess the potential skin irritation, and a 10% (w/v) aqueous solution of sodium dodecyl sulfate (SDS) was used as a positive control in each animal. The dorsal skin of each animal was shaved carefully and divided into 3 different sections with each area of 9 cm^2. Before the experiment, the initial EI values of the selected sites were determined as the baseline value for normalization. ISO, ISO-10 and 10% SDS of 500 μL were respectively applied on the shaved skin, which was then covered with a sheet of double-layer gauze to prevent any skin damage. After exposure of 4 h, the excess solution was removed and the application site was gently cleaned with a water soaked cotton wool swab. At different intervals, EI was determined automatically, and the baseline values were subtracted from the achieved measurements to give the actual changes (ΔEI) in the skin erythema. The experiments were performed in quadruplicates.

Statistical Analysis

Results are expressed as mean ± S.E. The data were subjected to analysis of variance (ANOVA) using SPSS 16.0 software. A significant level was taken as $P<0.05$.

RESULTS

Volatility of ISO and Its Long-Chain Esters

At the temperature of 50°C, ISO exhibited the highest volatilization rate (1.89 $mg^{-1} \cdot h^{-1} \cdot cm^{-2}$) among the tested compounds. Among the esters, the most volatile one was ISO-C6 (0.34 $mg^{-1} \cdot h^{-1} \cdot cm^{-2}$), which was followed by ISO-C8 (0.18 $mg^{-1} \cdot h^{-1} \cdot cm^{-2}$), ISO-C10 (0.15 $mg^{-1} \cdot h^{-1} \cdot cm^{-2}$), ISO-C12 (0.08 $mg^{-1} \cdot h^{-1} \cdot cm^{-2}$), ISO-C14 (0.05 $mg^{-1} \cdot h^{-1} \cdot cm^{-2}$) and ISO-C16 (0.03 $mg^{-1} \cdot h^{-1} \cdot cm^{-2}$). These results suggested that the long chain esters of ISO were less volatile than ISO.

Permeation Enhancement Effect

Skin Permeation of AM

Figure 2a shows the ER values of ISO and its long-chain esters towards the permeation parameters of AM. Compared with control, the skin permeation of AM was greatly promoted by the synthesized long-chain esters ($P<0.05$), whereas ISO exhibited no significant effect ($P>0.05$). A parabolic relationship was found between the enhancing activity and the carbon number of the long-chain esters. The maximum activities were observed with ISO-C10 and ISO-C12, with ER values of 2.81 and 2.71, respectively. The lowest active enhancer was ISO-C6, which could still increase the Q_{8h} of AM by 2.00-fold in comparison with the control. The partition coefficients (K') and diffusion coefficients (D') of AM in the presence of different ISO esters are presented in Fig. 2b. As shown, increasing the chain length from 8 carbons to 16 carbons improved the D' but reduced the K' for the drug permeation. Compared with control, the shortest ISO-C6 only produced a mild increase in K', but hardly had any effect on D'. Other permeation parameters and the drug solubility in the donor vehicle are shown in Supplementary Material.

Enhancing effect of saturated fatty acids and their mixtures with ISO were also investigated, and the results were present in Fig. 3. Compared with control, hexanoic acid (6-AC) neither promote nor retard the transdermal absorption of AM. However, with increasing the carbon chain length of the saturated fatty acids, significant retarding effect was observed ($ER<1$), and combination with ISO did not either change the retarding effect of the saturated fatty acids.

Skin Permeation of FP

The enhancing effects of ISO esters on the permeation of FP are presented in Fig. 4a. In contrast to control, ISO exhibited a slight but significant enhancement effect on the percutaneous absorption of FP, providing an ER of 1.35 ($P<0.05$). As for the long-chain esters, ISO-C6 had no influence on the skin permeation of FP ($P>0.05$). However, upon the chain lengths changed over the range of 8 carbons to 14 carbons, except for ISO-C12, the enhancement effects of the synthesized compounds were greatly increased and significantly higher than that of ISO ($P<0.05$). Especially, the ISO-C8, ISO-C10 and ISO-C14 could all increase the cumulative penetrated amount of FP with about 2.2 folds as much as that of the control group. With the chain length further increasing to 16 carbons, the permeation enhancement effect was slightly decreased, but still significantly higher than that of ISO ($P<0.05$). The K' and D' of FP in the presence of different ISO esters are presented in Fig. 4b. With prolonging the chain length from 8 carbons to 16 carbons, similar trends as observed with AM were found in the

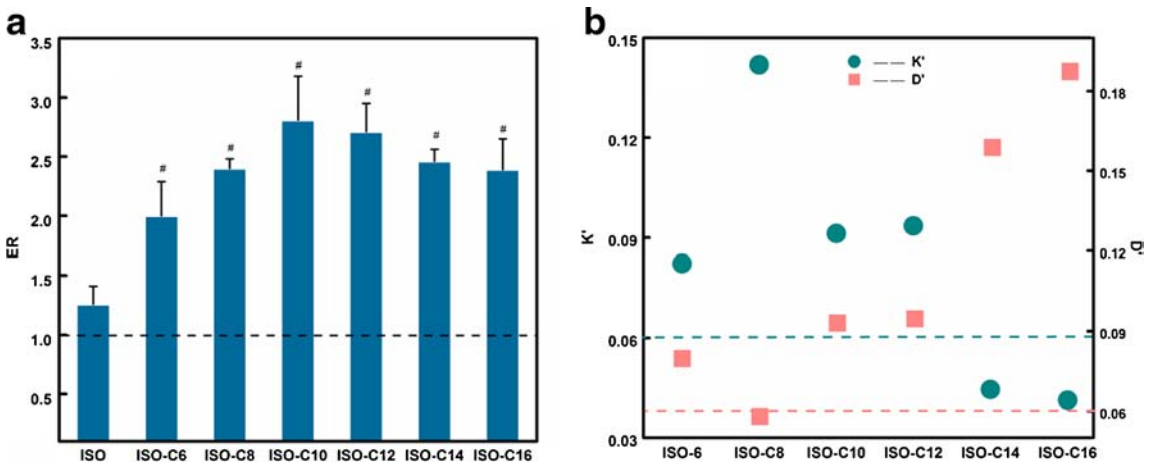

Fig. 2 (**a**) The ER values of ISO and its esters towards the permeation of AM. Data are presented as the mean ± S.E. ($n=4$). The dotted line represents the enhancement effect of the blank control (ER = 1), # represents the ER significantly higher than the control and ISO ($P<0.05$). (**b**) The apparent partition coefficient (K') and diffusivity coefficient (D') of AM permeated through the excised rat skin, when different long chain esters of ISO were used as the permeation enhancers. The *green* and *red* dotted lines respectively represent the K' and D' in the control group.

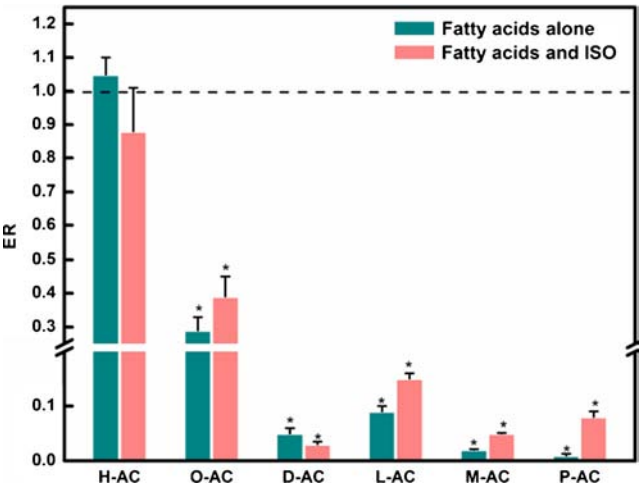

Fig. 3 The ER values of saturated fatty acids towards the permeation of AM. Data are presented as the mean ± S.E. ($n=4$). The dotted line represents the enhancement effect of the blank control (ER = 1), * represents the ER significantly lower than the control ($P<0.05$).

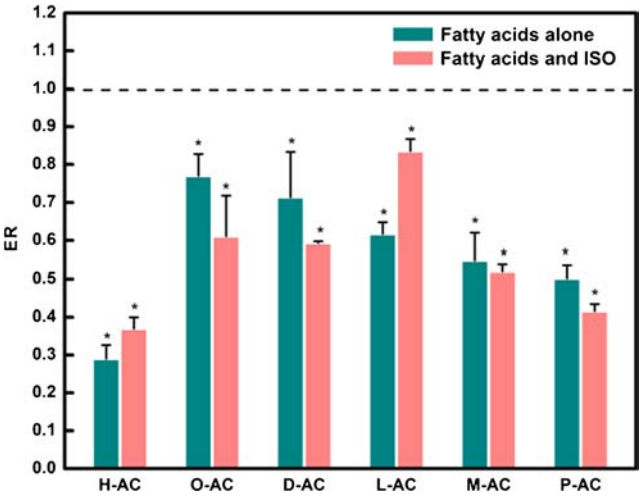

Fig. 5 The ER values of saturated fatty acids towards the permeation of FP. Data are presented as the mean ± S.E. ($n=4$). The Dotted line represents the enhancement effect of the blank control (ER = 1), * represents the ER significantly lower than the control ($P<0.05$).

K′ and D′ of FP. Other permeation parameters and the drug solubility are shown in Supplementary Material.

The effects of saturated fatty acids and their physical mixtures with ISO on the transdermal permeability of FP are illustrated in Fig. 5. Similarly, all the fatty acids in the present study significantly reduce the percutaneous absorption of FP ($ER<1$), whether or not combined with ISO.

In consideration of the similar activities of the compounds with different chain length, only decanoic acid (DA) and its ester (ISO-C10) were selected in further studies.

CLSM Analysis

In the study, we examined the rat skin samples subsequent to the application of (a) solvent blank, (b) ISO, (c) DA, (d) ISO and DA, and (e) ISO-C10. The xz optical sections of the skin after treatment with fluorescein solutions in different groups are shown in Fig. 6. The auto fluorescence property of the skin was not observed at the selected wavelength of 488 nm. The morphology of the surface layers identically confirmed with the reported "brick and mortar" of the SC, and the flat hexagonal structure of the horny cells was clearly observed at the skin surface (19). In specific, in the control group, it was shown that fluorescein could penetrate into the skin up to 30 μm without addition of any permeation modifiers (Fig. 6a). When the ISO solution was administrated, no obvious increase in permeation depth was observed, indicating that ISO had little effect on the permeation of fluorescein (Fig. 6b). However, upon the application of D-AC or its mixture with ISO, the fluorescein

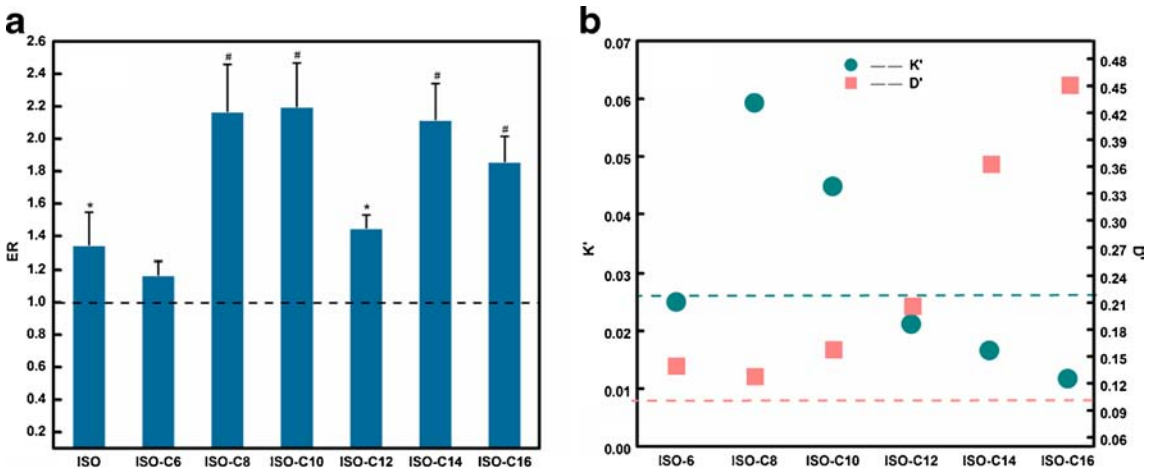

Fig. 4 (**a**) The ER values of ISO and its esters towards the permeation of FP. Data are presented as the mean ± S.E. ($n=4$). The Dotted line represents the enhancement effect of the blank control (ER = 1), # represents the ER significantly higher than that both of the control and ISO ($P<0.05$), and * represents the ER only higher than the control group ($P<0.05$). (**b**) The apparent partition coefficient (K') and diffusivity coefficient (D') of FP permeated through the excised rat skin, when different long chain esters of ISO were used as the permeation enhancers. The *green* and *red* dotted lines respectively represent the K' and D' in the control group.

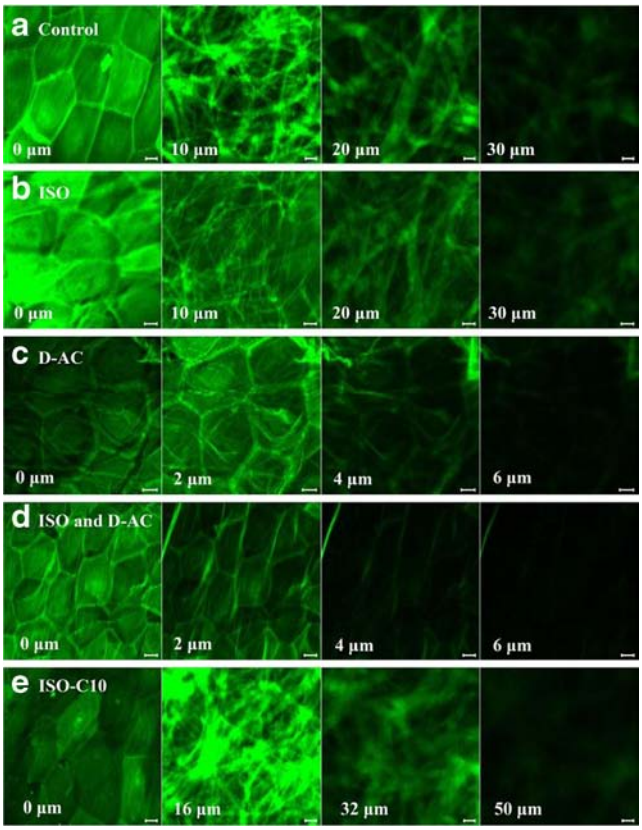

Fig. 6 CLSM images of the rat skin after the treatment by IPM solution for 20 min with or without penetration modifiers. (**a**) Solvent blank, (**b**) ISO, (**c**) DA, (**d**) physical mixture of ISO and DA, and (**e**) ISO-C10. Scale bar represents 10 μm.

permeation was significantly inhibited, and the florescent probe was only observed within 6 μm in depth of the rat skin (Fig. 6c and d). By contrast, a significant increase in the skin deposition of fluorescein was observed with the skin segment treated with ISO- C10, where the fluorescein could be found up to a depth of 50 μm (Fig. 6e). This result substantiated the observation from the *in vitro* permeation experiments.

ATR-FTIR Analysis

To further investigate the impact of an enhancer or a retarder on the molecular organization of the lipids in the SC, ATR-FTIR measurements were conducted. The absorption frequencies from the methylene asymmetric stretching vibration (v_{as} CH_2, ~2,920 cm^{-1}), symmetric stretching vibration (v_s CH_2, ~2,850 cm^{-1}), amide I (~1,650 cm^{-1}) and amide II (~1,550 cm^{-1}) bands were observed, and the wave numbers of these absorption peaks were listed in Table 1. For the untreated control sample, the CH_2 symmetric and asymmetric vibration bands were respectively observed at the wave numbers of 2918.27 ± 0.28 cm^{-1} and 2849.93 ± 0.10 cm^{-1}. Treatment of the skin with ISO alone produced no significant shift in these two absorption peaks. However, in the presence of DA, both of them moved to lower wave numbers, and the peak position of the CH_2 asymmetric vibration would be further decreased when DA and ISO were applied together on the skin. By contrast, only ISO-C10 shifted the CH_2 symmetric and asymmetric vibration towards the higher wave numbers, which could be respectively observed at 2920.81 ± 0.43 and 2850.93 ± 0.20 cm^{-1}. On the other hand, the amide I and amide II absorption peaks were also observed, but neither of them exhibited significant shift in the presence of the above mentioned permeation modifiers.

Skin Irritation

In Vitro Cytotoxicity (MTT Assay)

The cell viabilities of keratinocytes and fibroblasts after treatment with various concentrations of the two compounds are respectively shown in Fig. 7a and b. Following 24 h incubation, ISO and ISO-C10 showed dose-dependent cytotoxicity on the keratinocytes and fibroblasts. However, both of them did not induce a 50% reduction in the cells viability up to the high dosage of 3 mmol/L. No significant difference was observed between the cytoxicity of ISO and ISO-C10, however, the trend of decrease in the cytoxicity to both of the two cell lines by ISO-C10 was indicated by comparison with ISO. These results suggested that esterification of ISO would not produce additional toxicity towards the skin cells.

In Vivo Skin Irritation

As shown in Fig. 8, after treatment of SDS, ISO and ISO-C10, the skin erythema was significantly increased, suggesting that the rabbit could respond adequately to the skin irritants. The greatest skin color change was provided by SDS, and this effect was not declined at all throughout the experiment. There was no significant difference between ISO and ISO-C10, and about 12 h was required for the enhancer treated skin to achieve the complete skin recovery. The irritation experiments demonstrated that ISO and ISO-C10 could both slightly increase the skin erythema, but their action would be easily reversible.

DISCUSSION

In this study, the influence of the prepared compounds in drug skin permeation was investigated using IPM as a donor vehicle. IPM is a non-polar aprotic solvent which is commonly used in pharmaceutical and topical formulations as a hydrophobic carrier (20). It has a great solubility to the highly lipophilic compounds, so that the studied saturated fatty acids and their esters can be fully dissolved in it (7).

It was indicated that the efficiency of the permeation enhancers was drug specific (21), which was also found in the

Table I Peak Positions of the Absorption Bands in ATR-FTIR Spectra from Different Samples

Each value represents the mean ± S.E. (n = 3)

* represents the values significantly different form that of the control ($p < 0.05$)

Samples	v_{as} CH_2 (cm^{-1})	v_s CH_2 (cm^{-1})	Amide I (cm^{-1})	Amide II (cm^{-1})
Control	2918.27 ± 0.28	2849.93 ± 0.10	1646.55 ± 0.25	1544.44 ± 0.22
ISO	2918.10 ± 0.04	2849.68 ± 0.06	1646.12 ± 0.23	1544.24 ± 0.25
DA	2917.06 ± 0.16*	2848.94 ± 0.03*	1646.25 ± 0.27	1544.80 ± 0.35
ISO & DA	2916.71 ± 0.15*	2848.93 ± 0.01*	1646.64 ± 0.06	1544.52 ± 0.22
ISO-C10	2920.81 ± 0.43*	2850.93 ± 0.20*	1646.70 ± 0.14	1544.30 ± 0.18

present study. As shown in Fig. 2a, the effect of the long-chain esters on the permeation of AM showed a parabolic dependence on their carbon chain length, with maximum peaks of 10–12 carbons. However, consistent result was not observed on FP, in which, the medium-chain ISO-C12 rather resulted in a lower activity than the other esters (Fig. 4a). To illustrate the regulation of the enhancers in the skin permeability towards different drugs, the partition and diffusion coefficients of AM and FP through the skin with or without the tested compounds as enhancers were respectively determined. As shown in Fig. 2b and b, the esters with shorter chain length mainly increased the K' values of the two drugs, while the esters with longer chain length increased the D' values. In the case of medium-chain ISO-C12, it could greatly increased the permeation of AM via a dual enhancement effect both on the D' and on the K' of the drug. By contrast, its promoting activity towards the permeation of FP was much lower, which might be partly attributed to its single enhancement on the D', without affecting the K' of the drug. Furthermore, in the presence of the shortest chain ester (ISO-C6), both of D' and K' showed less increase than other esters, which would also result in a reduction or even disappearance of enhancing activity.

CLSM was utilized to visualize the permeation of exogenous molecule in the skin under the influence of the permeation modifiers. Since the drugs, FP and AM, had no fluorescence and could not be visualized by CLSM, a substitute probe (fluorescein) that was often studied in transdermal delivery was used instead.

Rat abdominal epidermis was a 32-μm hydrophobic layer, providing an efficient permeation obstacle for exogenous molecules (22). According to the result of CLSM, it was suggested that the fluorescein in the control group localized throughout the epidermis of the skin, but did not extended into the deeper tissue layers. In the group of ISO-C10, the flurescence probe was clearly observed beyond the epidermis and into the dermal layer, which indicated that ISO-C10 could effectively breach the barrier function of the epidermis and increase the skin permeability. However, for the skin treated with DA or its mixture with ISO, the fluorescein was only deposited in the upper layer of the epidermis, i.e. the SC. Obviously, both of the *in vitro* permeation experiments and the CLSM study indicated a negative influence of the saturated fatty acid on the skin permeability.

Although saturated fatty acids were reported to enhance the transdermal permeation of several drugs, their main mechanisms of action were simply attributed to the increase of drug solubility in the donor vehicle (23), improvement of adhesion properties as a tackifier agent (24), or synergistic action with cosolvents, e.g., propylene glycol (25). The sole effect of saturated fatty acids on the biophysical structure of the skin was rarely studied, and current understanding about their influence in TDDS was limited as well (26).

In the present study, ATR-FTIR experiments were carried out to probe the retarding action of the saturated fatty acids, as well as to investigate the possible enhancement mechanism of the long-chain ISO esters. As a probe-free and noninvasive

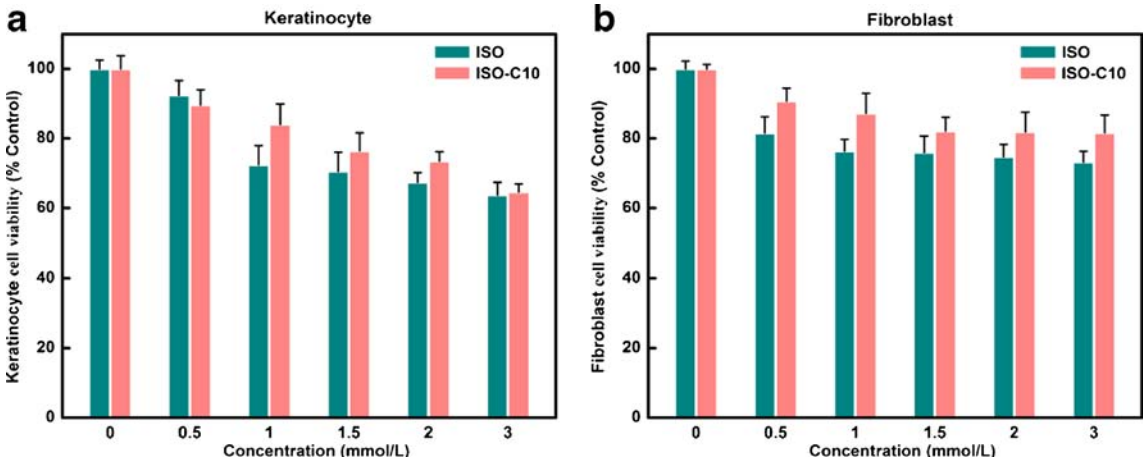

Fig. 7 Cell viability of keratinocyte (**a**) and fibroblast (**b**) after treatment of ISO and ISO-C10 at different concentrations. Data are presented as the mean ± S.E. ($n = 4$).

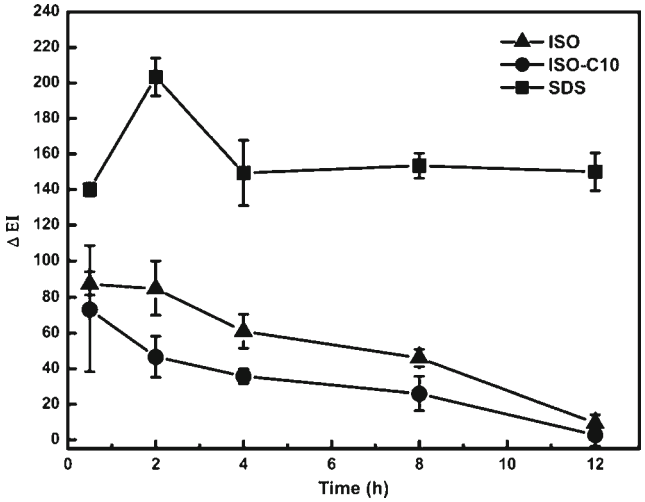

Fig. 8 ΔEI values of the rabbit skin after the treatment of ISO, ISO-C10 and SDS. Data are presented as the mean ± S.E. ($n=4$).

technique, ATR-FTIR is a powerful tool to study the mechanisms of the action of the permeation enhancers. In the infrared spectra of skin, the CH_2 asymmetirc and symmetric vibrations were derived from the methylene groups on the alkyl chain of the intercellular lipids in SC, and the amide I and II belonged to the amide bonds of the keratin in corneocytes (19). The displacement of amide I and II to lower wave numbers was always examined to suggest the changes of keratin structure in SC (27). In the present study, no significant changes were observed in the peak positions of the two absorption bands, which indicated that the studied compounds mainly targeted the SC lipid domain but not the protein domain for the permeation enhancement or retardation.

The CH_2 symmetric and asymmetric stretching frequencies have often been used to study the alternations of SC lipid hydrocarbon chain packing and possible conformational changes induced by chemical enhancers (28). The two bands are shifted to lower wave numbers (i.e. red shift) for all-trans conformation of the alkyl groups, and to higher values as gauche conformers are introduced along the chains (a process called rotamer disordering). An increase in the number of the gauche conformers in the lipid would result in an increased mobility of the lipid alkyl chains (29). In the present study, ethanol was used as a suitable solvent, mainly due to its little effect on C-H stretching absorbance, as well as its rapid evaporation on the skin (30,31).

The ATR-FTIR results indicated that treatment of rat skin with ISO alone did not produce any significant change in the peak positions of CH_2 asymmetirc and symmetric vibrations, which indicated that ISO could hardly influence the molecular organization of the alkyl chains in SC lipids. Similar results were also found in previous studies for other terpenes such as eugenol and menthone (32,33). It was proposed that these compounds might uptake into the protein domain or be pooled in the polar interface between the multiple lipid bilayers, without affecting the hydrophobic region in SC (34,35). Our previous investigation also revealed that terpenes only interacted with the polar moieties of the intercellular lipids via H-bonds, and almost had no effect on the stretching vibration of methylene in the alkyl tails of the lipids (36).

Skin application of saturated fatty acid (DA) or its mixture with ISO produced an overall decrease in the wave numbers of CH_2 asymmetirc and symmetric vibrations, while a similar experiment with its ester (ISO-C10) led to an apparent increase in these two peak positions. These totally distinct changes might result in their different effects on the skin permeability. However, such a conclusion might arise from the overlapping of the SC lipids and the external materials that also contained a hydrophobic chain in their structures. The individual effect of saturated fatty acids or their esters on the packing of the SC lipids was unknown, and it would be of particular importance to understand whether these molecules really inserted their hydrophobic tails into the intercellular lipid bilayers to influence the lipid order, or only existed in another phase in the SC lipids.

The lipid matrix of SC was composed of ceramides, cholesterol and long-chain free fatty acids, such as palmitic acid (PA). Mao *et al.* demonstrated that PA and ceramide existed in different phases in the SC lipids, and PA was more ordered than the ceramides. Disturbance effect of a fluid-like enhancer, e.g. ISO-C10, would more likely occur in the domains of ceramides (37). Incorporation of such enhancers into lipid domains would cause increased lipid fluidity as well as phase separation, and either of these effects would result in higher skin permeability (30,38). By contrast, the domain of PA was less likely to be influenced by permeation enhancers, and it might play an essential role in maintaining the barrier function of the skin (37). Cotte *et al.* reported that saturated fatty acids (PA and MA) applied on the skin would prefer an ordered conformation to exist in the SC lipids of the skin, which agreed well with the result of our study (39). It was probably because that saturated fatty acids tend to remain in the more ordered PA domain that was much more similar to their stable conformation. Over all, the different effects of saturated fatty acids and their esters would be due to their respective effect on the different lipid domains. Saturated fatty acids might exist in the ordered lipid domain to increase the barrier function of the skin, while the long chain esters might partition into the less ordered lipid domain to produce the permeation effect.

CONCLUSION

Saturated long-chain esters of ISO was shown to be promising candidates as permeation enhancers for clinical transdermal drug delivery, with the advantages of high efficiency, low volatility, low skin irritation and toxicity. It was suggested that

chemical linkage of saturated fatty acids with ISO was critical for the enhancement activity. Covalent attaching of long hydrophobic chain to a polar cycle molecule might be a promising strategy to design novel and potent permeation enhancers for promoting the percutaneous absorption of drugs.

ACKNOWLEDGMENTS AND DISCLOSURES

This work was supported by the National Natural Science Foundation of China (No: 81173007). The authors report no declarations of interest.

REFERENCES

1. Prausnitz MR, Langer R. Transdermal drug delivery. Nat Biotechnol. 2008;26:1261–8.
2. Hrabálek, Doležal P, Vávrová K, Zbytovská J, Holas T, Klimentová J, *et al.* Synthesis and enhancing effect of transkarbam 12 on the transdermal delivery of theophylline, clotrimazole, flobufen, and griseofulvin. Pharm Res. 2006;23:912–9.
3. Doležal P, Hrabálek A, Semecký V. ε-Aminocaproic acid esters as transdermal penetration enhancing agents. Pharm Res. 1993;10: 1015–9.
4. Karande P, Jain A, Ergun K, Kispersky V, Mitragotri S. Design principles of chemical permeation enhancers for transdermal drug delivery. Proc Natl Acad Sci U S A. 2005;102: 4688–93.
5. Jampilek J, Brychtova K. Azone analogues classification, design, and transdermal permeation principles. Med Res Rev. 2012;32:907–47.
6. Vávrová K, Hrabálek A, Dolezal P, Holas T, Klimentová J, Novotný J. Biodegradable derivatives of tranexamic acid as transdermal permeation enhancers. J Control Release. 2005;104:41–9.
7. Zhao L, Fang L, Xu Y, Liu S, He Z, Zhao Y. Transdermal delivery of penetrants with differing lipophilicities using O-acylmenthol derivatives as permeation enhancers. Eur J Pharm Biopharm. 2008;69: 199–213.
8. Vávrová K, Zbytovská J, Hrabálek A. Amphiphilic transdermal permeation enhancers: structure-activity relationships. Curr Med Chem. 2005;12:2273–91.
9. Ishida K, Obata Y, Takayama K. Trandermal absorption promoter, and external skin formulation thereof. 2011;WO 2011158964.
10. Aungst BJ. Structure/Effect studies of fatty acid isomers as skin permeation enhancers and skin irritants. Pharm Res. 1989;6: 244–7.
11. Karande P, Mitragotri S. Enhancement of transdermal drug delivery via synergistic action of chemicals. Biochim Biophys Acta. 2009;1788:2362–73.
12. Sun Y, Fang L, Zhu M, Li W, Meng P, Li L, *et al.* Drug-in-adhesive transdermal patch for S-Amlodipine free base: in vitro and in vivo characterization. Int J Pharm. 2009;382:165–71.
13. van der Geest R, Elshove DAR, Danhof M, Lavrijsen APM, Boddé HE. Non-invasive assessment of skin barrier integrity and skin irritation following iontophoretic current application in humans. J Control Release. 1996;41:205–13.
14. Ma X, Fang L, Guo J, Zhao N, He Z. Effect of counter-ions and permeation enhancers on the skin permeation of flurbiprofen. J Pharm Sci. 2010;99:1826–37.
15. Williams AC, Barry BW. Terpenes and the lipid-protein-partitioning theory of skin permeation enhancement. Pharm Res. 1991;8:17–24.
16. Alvarez-Román R, Naik A, Kalia YN, Guy RH, Fessi H. Enhancement of topical delivery from biodegradable nanoparticles. Pharm Res. 2004;21:1818–25.
17. Sugibayashi K, Watanabe T, Hasegawa T, Takahashi H, Ishibashi T. Kinetic analysis on the in vitro cytotoxicity using living skin equivalent for ranking the toxic potential of dermal irritants. Toxicol In Vitro. 2002;16:759–63.
18. Nose T, Tsurumi K. Pharmacological studies on cutaneous inflammation induced by ultraviolet irradiation (1): quantification of erythema by reflectance colorimetry and correlation with cutaneous blood flow. Jpn J Pharmacol. 1993;62:245–56.
19. Obata Y, Utsumi S, Watanabe H, Suda M, Tokudome Y, Otsuka M, *et al.* Infrared spectroscopic study of lipid interaction in stratum corneum treated with transdermal absorption enhancers. Int J Pharm. 2010;389:18–23.
20. Lau WM, White AW, Heard CM. Topical delivery of a naproxen-dithranol co-drug: in vitro skin penetration, permeation, and staining. Pharm Res. 2010;27:2734–42.
21. Williams AC, Barry BW. Penetration enhancers. Adv Drug Deliv Rev. 2004;56:603–18.
22. Godin B, Touitou E. Transdermal skin delivery: predictions for humans from in vivo, ex vivo and animal models. Adv Drug Deliv Rev. 2007;59:1152–61.
23. Choi J, Choi MK, Chong S, Chung SJ, Shim CK, Kim DD. Effect of fatty acids on the transdermal delivery of donepezil: in vitro and in vivo evaluation. Int J Pharm. 2012;422:83–90.
24. Carrara D, Alres B. Transdermal patch comprising a combination of two or more fatty acids or alcohols as permeation enhancers, a tackifier agent and a cohesion improver to improve adhesion properties. 1998;EP 0913158 B1.
25. Kim MJ, Doh HJ. Skin permeation enhancement of diclofenac by fatty acids. Drug Deliv. 2008;15:373–9.
26. Ibrahim SA, Li SK. Efficiency of fatty acids as chemical permeation enhancers: mechanisms and structure enhancement relationship. Pharm Res. 2009;27:116–25.
27. He W, Guo X, Xiao L, Feng M. Study on the mechanisms of chitosan and its derivatives used as transdermal penetration enhancers. Int J Pharm. 2009;382:234–43.
28. Ibrahim SA, Li SK. Chemical enhancer solubility in human stratum corneum lipids and enhancer mechanism of action on stratum corneum lipid domain. Int J Pharm. 2010;383: 89–98.
29. Guillard EC, Tfayli A, Laugel C, Baillet-Guffroy A. Molecular interactions of penetration enhancers within ceramides organization: a FTIR approach. Eur J Pharm Sci. 2009;36:192–9.
30. Bhatia KS, Gao S, Singh J. Effect of penetration enhancers and iontophoresis on the FT-IR spectroscopy and LHRH permeability through porcine skin. J Control Release. 1997;47: 81–9.
31. Ibrahim SA, Li SK. Effects of solvent deposited enhancers on transdermal permeation and their relationship with Emax. J Control Release. 2009;136:117–24.
32. Zhao K, Singh J. Mechanisms of percutaneous absorption of tamoxifen by terpenes: eugenol, d-limonene and menthone. J Control Release. 1998;1998(55):253–60.
33. Krishnaiah YSR, Satyanarayana V, Karthikeyan RS. Permeation enhancing effect of menthol on the percutaneous flux of nicardipine hydrochloride through excised rat epidermis from hydroxypropyl cellulose gels. Pharm Dev Technol. 2002;7: 305–15.

34. Cornwell PA, Barry BW. The routes of permeation of ions and 5-fluorouracil across human skin and the mechanisms of action of terpene skin permeation enhancers. Int J Pharm. 1993;94:189–94.
35. Cornwell PA, Barry BW, Bouwstra JA, Gooris GS. Modes of action of terpene permeation enhancers in human skin; differential scanning calorimetry, small-angle X-ray diffraction and enhancer uptake studies. Int J Pharm. 1996;127:9–26.
36. Chen Y, Wang J, Cun D, Wang M, Jiang J, Xi H, et al. Effect of unsaturated menthol analogues on the in vitro permeation of 5-fluorouracil through rat skin. Int J Pharm. 2013;443:120–7.
37. Mao G, VanWyck D, Xiao X, Mack Correa MC, Gunn E, Flach CR, et al. Oleic acid disorders stratum corneum lipids in Langmuir monolayers. Langmuir. 2013;29:4857–65.
38. Naik A, Pechtold LARM, Potts RO, Guy RH. Mechanism of oleic acid induced skin penetration enhancement in vivo in humans. J Control Release. 1995;37:299–306.
39. Cotte M, Dumas P, Besnard M, Tchoreloff P, Walter P. Synchrotron FT-IR microscopic study of chemical enhancers in transdermal drug delivery: example of fatty acids. J Control Release. 2004;97:269–81.